

## **Feasibility testing of 4D seismic monitoring with full-waveform tomography.**

Chad Hogan, Ken Hedlin, Gary Margrave, and Michael Lamoureux

### **ABSTRACT**

Full waveform tomography reveals subtle sub-wavelength perturbations in the velocity model, given a sufficiently accurate starting model. 4D seismic surveys over reservoirs are typically intended to detect small changes in a relatively well-known overall velocity field due to localized effects such as CO<sub>2</sub> injection, steam injection, petroleum production, and more. Full waveform tomography is ideally suited to detect and reveal the extent of these effects, both spatially and in terms of the magnitude of the effect on the velocity. Our early investigations strongly suggest that waveform tomography deserves serious consideration as a primary analysis tool for 4D seismic analysis.

### **INTRODUCTION**

Waveform tomography represents a natural extension of the concept of standard travel-time tomography. In this approach, the whole waveform of the transmitted signal is used in the imaging process, rather than simply the first arrival time. This method originated 25 years ago with the work of Lailly (1983), Tarantola (1984), and Mora (1987). It has been subsequently developed by many others, including Woodward (1992). Lately the primary champion of this method has been Gerhard Pratt and his research group. A subset of these publications includes Pratt (1990); Pratt and Worthington (1990); Pratt et al. (1998); Pratt (1999); Pratt and Shipp (1999); Sirgue and Pratt (2004); Brenders and Pratt (2006, 2007).

To date, applications of this method to the analysis of 4D seismic data have been sparse. We believe that this method is ideally suited to this analysis, however. In 4D analysis, it is common to have a well-established velocity model of the relevant geology, due to past surface seismic surveys, VSP investigations, and well-log data. The waveform tomography process requires a sufficiently accurate starting model, typically constrained by requiring that diving waves travelling from source to receiver in the starting model must be within a half wavelength of the actual recorded data (Pratt, 1999).

If it is possible to construct a velocity model that accurately models the first-arrival of seismic waveforms on a baseline survey, then it may be possible to use waveform tomography to analyze 4D changes in the imaged region. Small, subtle local perturbations to this velocity field should in principle be recoverable given sufficient data.

The purpose of this study is to investigate two major questions. First, is waveform tomography at all feasible for 4D monitoring? Second, if so, what acquisition parameters would maximize the effectiveness of this method?

### **FEASIBILITY TESTING ON SYNTHETIC DATA**

Our primary test model is a laterally-homogeneous section derived from the horizontal extension of a P-wave sonic log from the Pikes Peak field. This 2D model is displayed in

Figure 1. A perturbation of -500 m/s over an area of approximately 100 m horizontally and

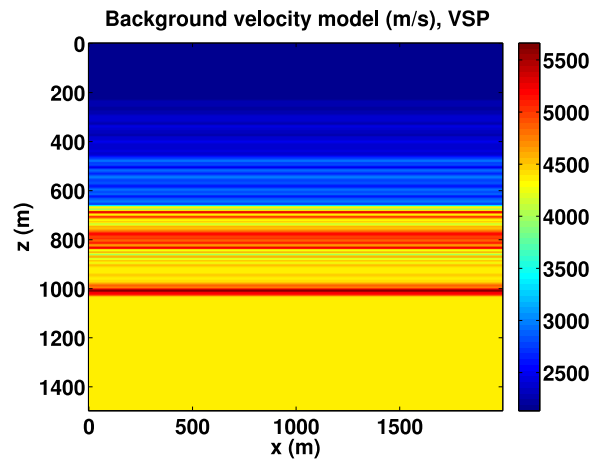


FIG. 1. Original velocity model with no 4D change.

30 m vertically is introduced to simulate the effect of steam injection or some other physical process with a similar net result on the seismic velocity of the region. This perturbation may be seen in Figures 2 and 3. Raytracing, shown in Figure 4, through a smoothed version of

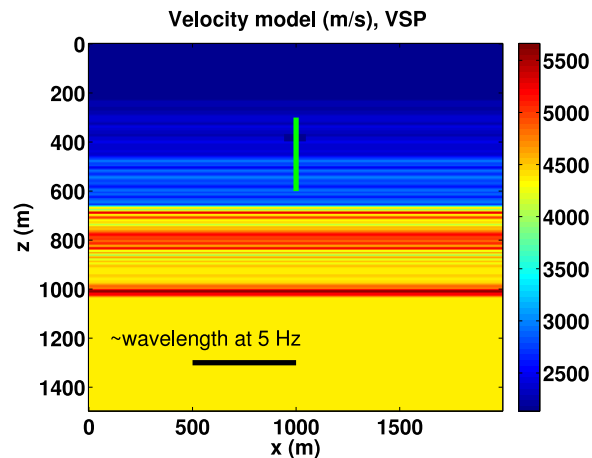


FIG. 2. Original velocity model plus steam-injection effect. The location of the VSP receivers is marked as a vertical green line at the injection site. The approximate wavelength at 5 Hz in the injected region is displayed for scale.

this velocity model reveals that our survey size is sufficient (barely) to capture the diving waves that pass through the perturbed region. Without this smoothing, these raypaths are reflected before they reach the target depth. This implies that only relatively low frequency diving waves will reach the target, and that the longest offsets will be required for inversion. (Hogan and Margrave, 2007). The model dimensions were constrained by computational limitations.

### Surface seismic modelling and inversion procedure

The forward modelling was performed on the perturbed model using a 2D acoustic frequency-domain finite difference code. This is the same forward-modelling code that is used in the inversion algorithm, and so is committing the so-called “inverse crime”. With

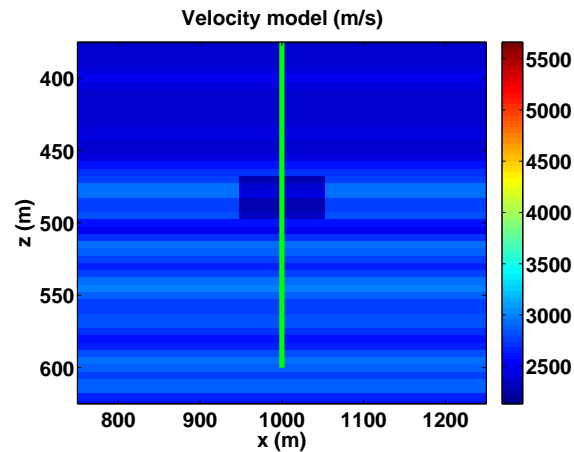


FIG. 3. Original velocity model plus steam-injection effect. The location of the VSP receivers is marked as a vertical green line at the injection site.

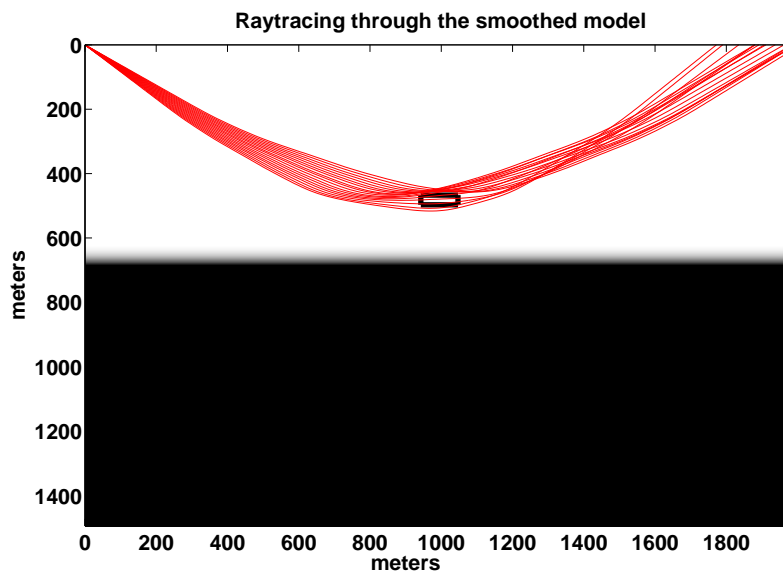


FIG. 4. Raytracing through the original model convolved with a 20 m Gaussian smoother

success using this algorithm, we intend to move beyond this to using external acoustic and elastic codes with future work. A sample time slice of this modelling is shown in Figure 5.

The simulated seismic surface reflection survey was recorded with receivers placed along the surface of the model at 10 m spacing. Sources were placed with 20 m spacing. Sources and receivers were located across the entire 2000 m extent of the survey.

The waveform tomography inversion was then performed using the original (unperturbed) background velocity model as its starting point. Constant-frequency inversions were carried out beginning at 5 Hz, and then using this result as input into a 6 Hz inversion. Although in many cases it is possible to use many (or few) frequencies to optimize the convergence (Sirgue and Pratt, 2004), for this inversion we found that results were best with an inversion beginning no higher than 5 Hz, and that beyond 6 Hz no appreciable

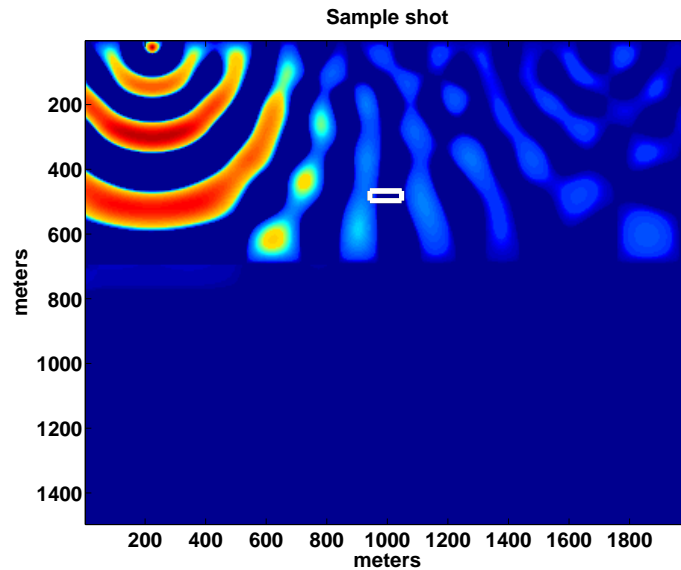


FIG. 5. Sample time slices of the forward-modelled data on the perturbed model. The white rectangle delineates the extent of the perturbation.

improvement was detectable.

All inversions were constrained to update the model within a region of 500 m by 500 m, centred at the anomaly. This stabilizes the inversion, and would be a reasonable (perhaps even overly conservative) constraint for the inversion of realistic data. This constrained region is shown in all difference plots of the inversion results.

### Surface seismic inversion results

The updated velocity model with the 5 Hz (Figure 6) and 5, 6 Hz (Figure 7) inversions are shown as a difference-plot with respect to the starting (background) velocity model, zoomed into the region of interest shown in Figure 2.

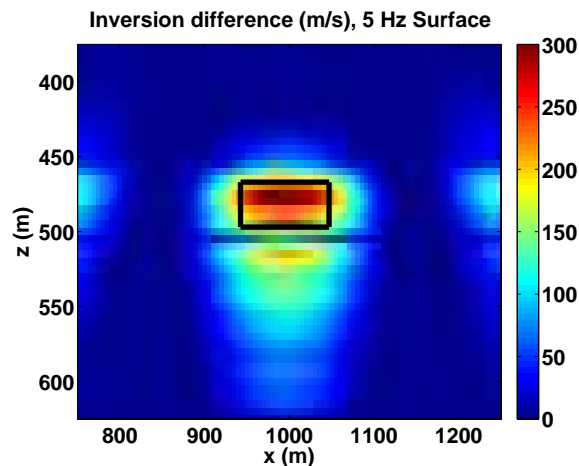


FIG. 6. The resulting surface-seismic velocity estimate from inversion at 5 Hz, as a difference from the starting (background) velocity model. Ideally, the amplitude of the perturbation would be exactly +500 m/s. One wavelength at 5 Hz would approximately span this entire displayed region at the velocity of the target region. The black box marks the spatial extent of the actual perturbation.

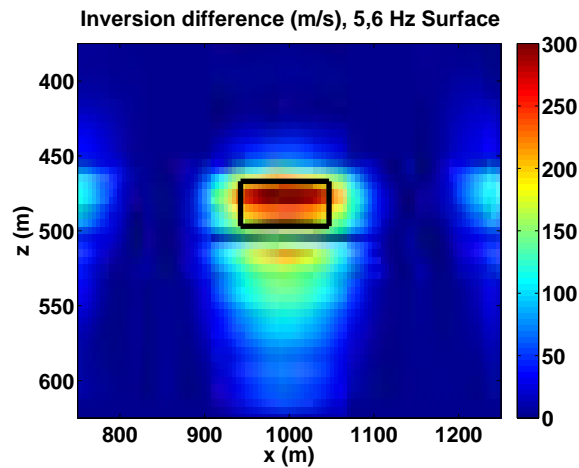


FIG. 7. The resulting surface-seismic velocity estimate from inversion at 5 Hz, as a difference from the starting (background) velocity model. Ideally, the amplitude of the perturbation would be exactly +500 m/s. One wavelength at 5 Hz would approximately span this entire displayed region at the velocity of the target region. The black box marks the spatial extent of the actual perturbation.

### VSP modelling and inversion procedure

The same starting velocity models were also used in a simulated VSP survey. In this survey, source locations across the 2000 m extent of the model were used at 20 m spacing. Receivers were placed in a borehole from 300 m to 600 m deep, at 10 m spacing. This well bore bisected the perturbed (steam-injection) site. This borehole is marked in green in Figure 2.

The updated velocity model with the 5 Hz and 5, 6 Hz inversions are shown in Figures 8 and 9 respectively, again as a difference-plot with respect to the starting (background) velocity model zoomed into the region of interest shown in Figure 2.

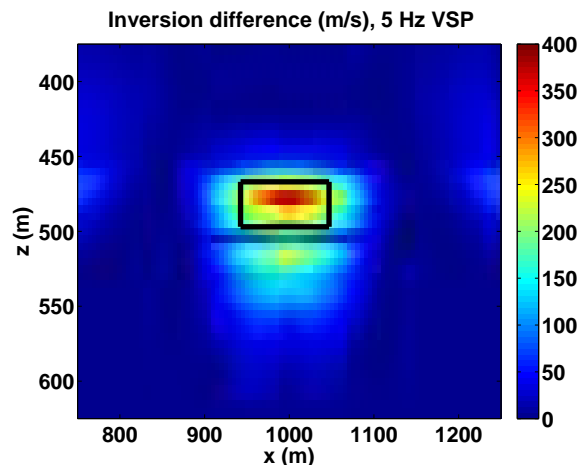


FIG. 8. The resulting VSP velocity estimate from inversion at 5 Hz, as a difference from the starting (background) velocity model. Ideally, the amplitude of the perturbation would be exactly +500 m/s. One wavelength at 5 Hz would approximately span this entire displayed region at the velocity of the target region. The black box marks the spatial extent of the actual perturbation.

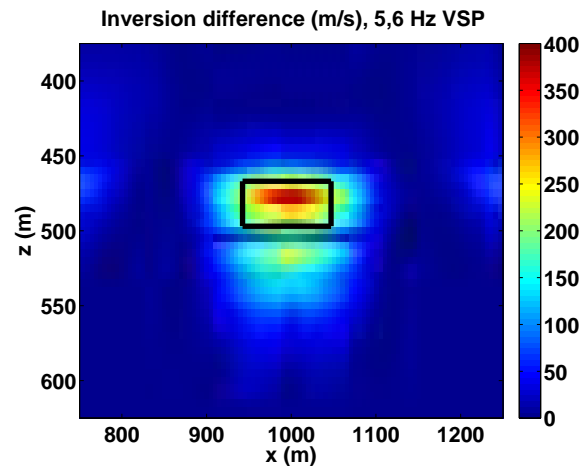


FIG. 9. The resulting VSP velocity estimate from inversion at 5 and 6 Hz, as a difference from the starting (background) velocity model. Ideally, the amplitude of the perturbation would be exactly +500 m/s. One wavelength at 5 Hz would approximately span this entire displayed region at the velocity of the target region. The black box marks the spatial extent of the actual perturbation.

## DISCUSSION OF THE RESULTS

The waveform inversion procedure is providing significant updates to the background velocity model at well below the wavelength scale. Both surface seismic and VSP approaches yielded useful updates to the model that were consistent with the true anomaly both in terms of spatial extent and in magnitude. Although the maximum amplitude of the anomaly ( $\sim 300$  m/s for the surface seismic, and  $\sim 400$  m/s for the VSP survey) is somewhat less than the true amplitude (500 m/s), this is not surprising as the discovered spatial extent of the anomaly is somewhat larger than the true anomaly.

Both images gained the most benefit from 5 Hz data, with some minor improvement with the addition of 6 Hz. Although it was hoped that higher frequencies would focus the image better, in practice, higher frequencies did not converge effectively within the region of constraint. We speculate that this is due to the higher frequency components of the wavefields reflecting off strong contrasts in shallower regions. This is currently being investigated with further modelling studies.

## CONCLUSIONS AND FUTURE WORK

The results we have seen strongly indicate that waveform tomography merits further investigation as a viable method for analyzing a 4D signal in seismic data. Both surface and VSP methods provided comparable images, with slightly better results from the VSP method.

Seismic source considerations are significant. First, this “ideal conditions” inversion required 5 Hz data. Although explosive-source surveys easily contain this frequency and lower, vibration-source surveys often begin their sweep at frequencies higher than 5 Hz.

Acquisition geometry is also significant. In this test case, raytracing revealed that only the longest offsets (nearly 2 km for a 500 m deep target) contributed significantly to the

inversion. Also, although VSP surveys with geophones directly in the zone of interest are useful for reflection surveys, and can in some cases provide more information than surface seismic, in this case there was very little difference in results. We speculate that a crosswell survey or a VSP in a nearby observation well, either providing many raypaths travelling through the zone of interest, will yield improved results.

There are many open issues that will be addressed in the near future. These are broadly grouped into at least two sections: modelling and inversion methods, and acquisition and practical concerns.

First, we intend to move beyond the forward-modelling tools built into the inversion software program. This will allow us to investigate the impact of elastic effects such as ground roll on the inversion procedure. Second, as we gain familiarity with the inversion software, we expect to fine-tune our procedure, and optimize the selected frequencies for the inversion following Sirgue and Pratt (2004).

In terms of acquisition and practical concerns, we have three main areas of focus for the near future. First, we hope to investigate the effect of shallower layers in shadowing the perturbations at higher frequencies. This may allow us to optimize acquisition geometries, including testing cross-well surveys, to allow broad-band signals to propagate effectively through the target region more easily. Second, we will investigate more practical scenarios for the inversion, such as beginning the inversion with a more realistic seismic-derived background velocity model rather than the “perfect” background velocity model used in this investigation, including random and coherent noise, unknown source waveforms, and unknown near-surface layers. Third, we will look to find the limitations of the method in terms of perturbation size and magnitude.

## ACKNOWLEDGEMENTS

We gratefully acknowledge generous support from Husky Energy, MITACS, and the sponsors of CREWES.

## REFERENCES

- Brenders, A. J., and Pratt, R. G., 2006, Full waveform tomography for lithospheric imaging: results from a blind test in a realistic crustal model.: *Geophysical Journal International*, **168**, 133–151.
- Brenders, A. J., and Pratt, R. G., 2007, Efficient waveform tomography for lithospheric imaging: implications for realistic, two-dimensional acquisition geometries and low-frequency data.: *Geophysical Journal International*, **168**, 152–170.
- Hogan, C. M., and Margrave, G. F., 2007, Ray-tracing and eikonal solutions for low-frequency wavefields, Tech. rep., CREWES Research Report.
- Lailly, P., 1983, The seismic inverse problem as a sequence of stack before migrations, *in* Bednar, J. B., Redner, R., Robinson, E., and Weglein, A., Eds., SIAM Philadelphia, Conference on Inverse Scattering: Theory and Application, 206–220.
- Mora, P. R., 1987, Nonlinear two-dimensional elastic inversion of multioffset seismic data.: *Geophysics*, **52**, 1211–1228.
- Pratt, R. G., 1990, Frequency domain elastic wave modeling by finite differences: A tool for cross-hole seismic imaging.: *Geophysics*, **55**, 626–632.

- Pratt, R. G., 1999, Seismic waveform inversion in the frequency domain, Part I: Theory and verification in a physical scale model.: *Geophysics*, **64**, 888–901.
- Pratt, R. G., Shin, C., and Hicks, G., 1998, Gauss-Newton and full Newton methods in frequency-space seismic waveform inversion: *Geophysical Journal International*, **133**, 341–362.
- Pratt, R. G., and Shipp, R. M., 1999, Seismic waveform inversion in the frequency domain, part II: Fault delineation in sediments using crosshole data.: *Geophysics*, **64**, 902–914.
- Pratt, R. G., and Worthington, M. H., 1990, Inverse theory applied to multi-source cross-hole tomography. part I: Acoustic wave-equation method.: *Geophysical Prospecting*, **38**, 287–310.
- Sirgue, L., and Pratt, R. G., 2004, Efficient waveform inversion and imaging: a strategy for selecting temporal frequencies.: *Geophysics*, **69**, 231–248.
- Tarantola, A., 1984, Inversion of seismic reflection data in the acoustic approximation.: *Geophysics*, **49**, 1259–1266.
- Woodward, M. J., 1992, Wave equation tomography: *Geophysics*, **57**, 15–26.